

# STARS

University of Central Florida  
STARS

Faculty Bibliography 2000s

Faculty Bibliography

1-1-2007

## Coherent pulse detection and multi-channel coherent detection based on a single balanced homodyne receiver

Wangkuen Lee  
*University of Central Florida*

Hoss Izadpanah  
*University of Central Florida*

Peter J. Delfyett  
*University of Central Florida*

Ron Menendez

Shahab Etemad

Find similar works at: <https://stars.library.ucf.edu/facultybib2000>  
University of Central Florida Libraries <http://library.ucf.edu>

This Article is brought to you for free and open access by the Faculty Bibliography at STARS. It has been accepted for inclusion in Faculty Bibliography 2000s by an authorized administrator of STARS. For more information, please contact [STARS@ucf.edu](mailto:STARS@ucf.edu).

### Recommended Citation

Lee, Wangkuen; Izadpanah, Hoss; Delfyett, Peter J.; Menendez, Ron; and Etemad, Shahab, "Coherent pulse detection and multi-channel coherent detection based on a single balanced homodyne receiver" (2007). *Faculty Bibliography 2000s*. 7344.  
<https://stars.library.ucf.edu/facultybib2000/7344>



# Coherent pulse detection and multi-channel coherent detection based on a single balanced homodyne receiver

Wangkuen Lee, Hoss Izadpanah, and Peter J. Delfyett

*The College of Optics & Photonics, Center for Research & Education in Optics & Lasers (CREOL),  
University of Central Florida, Orlando, Florida 32816-2700 USA.*

*Email: wangkuen@creol.ucf.edu, delfyett@creol.ucf.edu*

Ron Menendez and Shahab Etemad

*Telcordia Technologies, Red Bank, New Jersey 07701-5699 USA*

**Abstract:** The performance of coherent pulse detection (CPD) and multi-channel coherent detection (MCCD) based on a single dual-balanced homodyne receiver was experimentally demonstrated using a grating-coupled hybridly mode-locked semiconductor laser. Compared with direct detection, a high coherent gain of over 10 dB, as well as an SNR improvement of over 5 dB, was obtained in both detection schemes. Our experimental results have confirmed that the coherent detection processes in CPD and MCCD are nearly the same based on a square-root LO power dependence. Nevertheless, the MCCD scheme has shown an advantage in a path-length error over the CPD scheme, revealing 2~3 dB improvement in sensitivities.

©2007 Optical Society of America

**OCIS codes:** (060.2920) Homodyning; (060.1660) Coherent communications; (140.4050) Mode-locked lasers

---

## References and links

1. R. C. Menendez, P. Toliver, S. Galli, A. Agarwal, T. Banwell, J. Jackel, J. Young, and S. Etemad, "Network applications of cascaded passive code translation for WDM-compatible spectrally phase-encoded optical CDMA," *IEEE J. of Lightwave Technol.* **23**, 3219-3231 (2005).
2. A. Agarwal, P. Toliver, R. Menendez, S. Etemad, J. Jackel, J. Young, T. Banwell, B. Little, S. Chu, W. Chen, W. Chen, J. Hryniewicz, F. Johnson, D. Gill, O. King, R. Davidson, K. Donovan, and P. Delfyett, "Fully programmable ring-resonator-based integrated photonic circuit for phase coherent applications," *IEEE J. of Lightwave Technol.* **24**, 77-86 (2006).
3. W. Lee, M-T. Choi, H. Izadpanah, P. J. Delfyett, and S. Etemad, "Coherent homodyne pulse detection for a spectral phase-encoded optical CDMA system using synchronized mode locked lasers," *OAA/COTA 2006, OSA Topical Meetings, CFD6*, June 30 (2006).
4. P. J. Delfyett, S. Gee, M-T. Choi, H. Izadpanah, W. Lee, S. Ozharar, F. Quinlan, and T. Yilmaz, "Optical frequency combs from semiconductor lasers and applications in ultra wideband signal processing and communications," *IEEE J. of Lightwave Technol.* **24**, 2701- 2719 (2006).
5. W. Lee and P. J. Delfyett, "Dual mode injection locking of two independent modelocked semiconductor lasers," *IEE Electronics Letters* **40**, 1182- 1183 (2004).
6. G. L. Abbas, V. W. S. Chan, and T. K. Yee, "A dual-detector optical heterodyne receiver for local oscillator noise suppression," *IEEE J. of Lightwave Technol.* **LT-3**, 1110- 1122 (1985).
7. W. Lee, M-T. Choi, H. Izadpanah, and P. J. Delfyett, "Relative intensity noise characteristics of a frequency stabilized grating-coupled mode-locked semiconductor laser," *IEE Electron. Lett.* **42**, 1156- 1157 (2006).

---

## 1. Introduction

Spectral phase-encoded optical code division multiple access (SPE-OCDMA) systems are of interest as they can play a role in secure communications. Coherent detection techniques may be applied to SPE-OCDMA by exploiting synchronized mode-locked semiconductor lasers (MSLs) as phase-locked transmitters and local oscillators. [1-3].

The fixed phase relationship of the optical frequency combs of the MSLs facilitates spectral phase encoding capability [4]. In addition, the short time duration of the optical pulses from the MSL have the potential to provide high processing gain, defined as the bandwidth ratio between the data rate and the spectral bandwidth of the optical pulses, in the SPE-OCDMA system. In addition, optical frequency as well as phase synchronization of the MSLs can be easily achievable by means of simple injection locking techniques [5]. Therefore, the MSL is very suitable for SPE-OCDMA systems application. However, inherent mode partition noise of the MSL produces relatively large intensity noise of the optical pulses from the MSL, which can severely impair system performance, especially on systems utilizing simple ASK modulation signals. Utilizing a balanced optical receiver in which the photocurrents from two output branches are subtracted, the relative intensity noise (RIN) from the optical sources can be significantly reduced [6].

In this paper, by using a free-space balanced receiver with two large-area photodetectors, we demonstrate two homodyne detection schemes, called coherent pulse detection (CPD) and multi-channel coherent detection (MCCD), which can be practically applied to coherent receivers for the SPE-OCDMA system based on synchronized MSLs. In section 2, we present an external cavity grating-coupled MSL system and its characteristics on optical frequency combs and optical pulses. In section 3, we present the experimental setup of a coherent homodyne receiver system for CPD and MCCD. Finally, in section 4, we present a comparison of the experimental results of CPD and MCCD.

In both CPD and MCCD experiments, a high coherent gain with a significantly improved SNR was obtained due to synchronous signal selectivity compared with direct detection, showing the potential of strong multi-user interference rejection that enables the accommodation of a higher number of users in multi-user SPE-OCDMA systems.

## 2. External cavity grating-coupled mode-locked semiconductor laser system

In our experiment, an external cavity grating-coupled MSL system was configured to generate phase coherent optical frequency combs with a fundamental cavity frequency of 10 GHz.

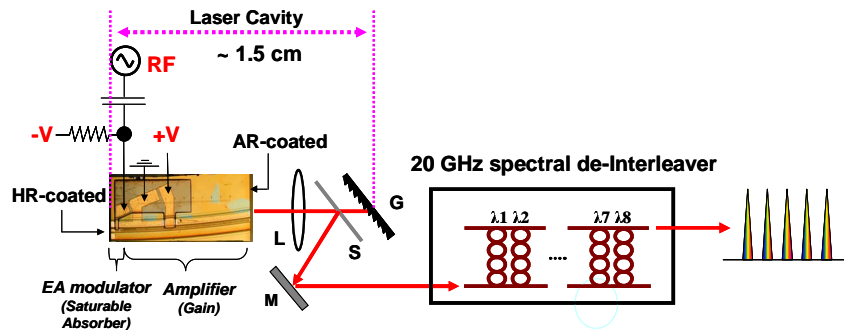


Fig. 1. Schematic of 10 GHz external cavity grating-coupled MSL system and a 20 GHz spectral de-interleaver (L: lens, S: optical sampler, G: grating, M: mirror)

Figure 1 shows the schematic of the mode-locked semiconductor laser (MSL) system that was used for the CPD and MCCD experiment. As shown Fig. 1, the laser cavity consists of an electroabsorption (EA) modulator incorporated two-section semiconductor optical amplifier (SOA), an aspheric collimating lens, an optical sampler, and a grating with a groove density of 600 lines/mm. The cavity length is approximately 1.5 cm which corresponds to a fundamental cavity frequency of 10 GHz. The MSL was hybridly mode-locked by applying a DC current of 79.23 mA on the gain section in the monolithic two-section device and a reverse bias of 2.72 V with a RF signal of 20 dBm at 10 GHz on the EA section of the device. Phase coherent optical frequency combs at 10 GHz are generated by establishing the optical

feedback between the high reflection (HR) coated device facet mirror and the grating. Subsequently, the 10 GHz MSL output was sent into a 20 GHz micro-ring resonator spectral de-interleaver to select every other laser line as shown in Fig. 1. It should be mentioned that the use of the 20-GHz channel spacing is to make a complete channel separation considering the resolution of gratings in the following MCCD experiment. More details are described in section 3.

Figure 2(a) shows the optical spectrum of the 10 GHz MSL. A 3-dB spectral bandwidth was measured to be 0.45 nm. Figure 2(b) shows the filtered frequency channels of the MSL after the 20 GHz de-interleaver. Figure 3 and Fig. 4 show sampling oscilloscope traces and intensity autocorrelation measurements corresponding to the optical spectra shown in Fig. 2, respectively. As shown in Fig. 4(a), the pulse duration directly from the MSL was measured to be 16.3 ps (assuming hyperbolic secant pulse shape).

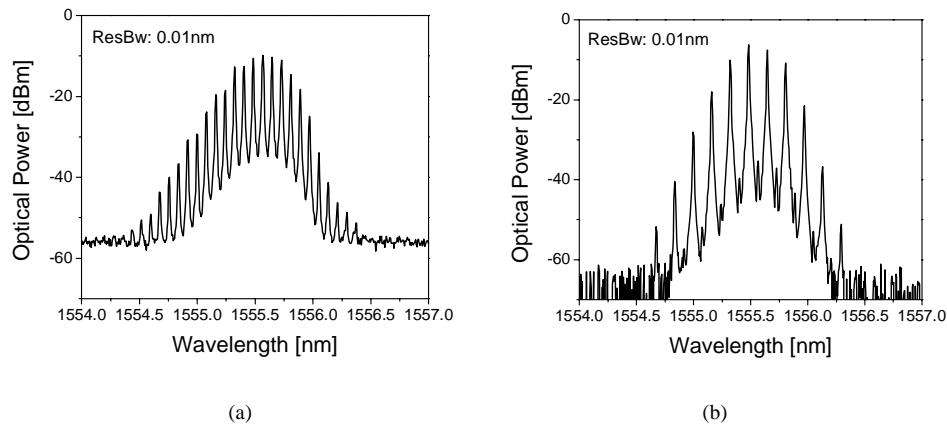


Fig. 2. Optical spectra: (a) optical spectrum of the 10 GHz hybridly MSL (b) optical spectrum of 10 GHz hybridly MSL after filtering through the 20 GHz de-interleaver.

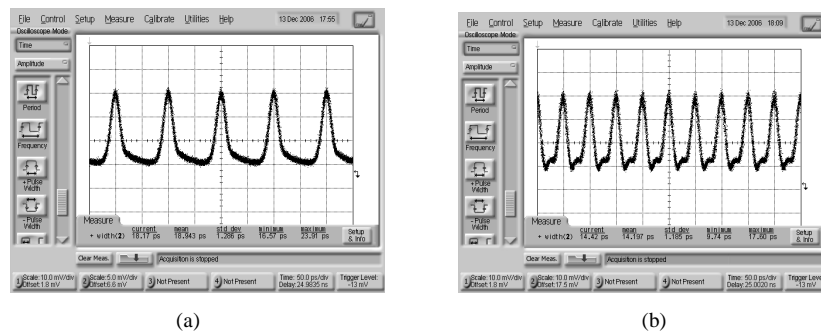


Fig. 3. Sampling oscilloscope traces: (a) pulse train of the 10 GHz hybridly MSL (b) 20-GHz pulse train after the 20 GHz de-interleaver (detector bandwidth is 50 GHz).

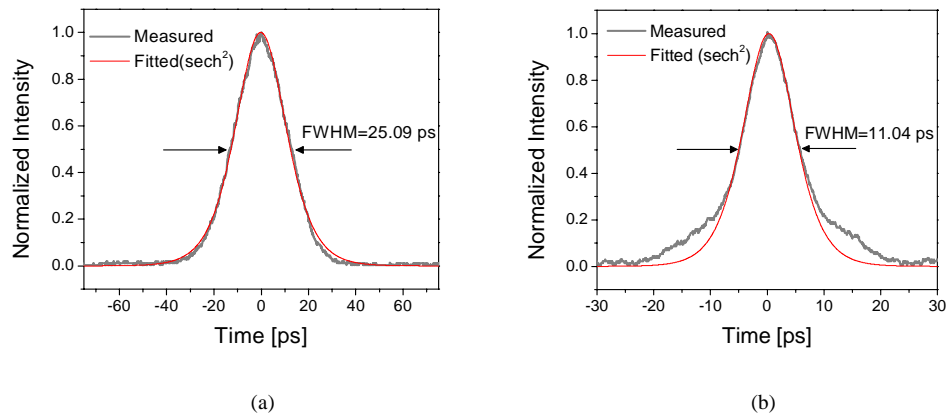


Fig. 4. Intensity autocorrelation measurements: (a) the optical pulse from the 10 GHz hybridly MSL (b) the optical pulse after 20 GHz de-interleaver

The time-bandwidth product was 0.9, which indicated that the measured pulse width is 2.9 times larger than the transform-limited pulse width. The relative intensity noise of the laser output was measured to be -150 dB/Hz [7]. The pulse duration after the 20 GHz de-interleaver was measured to be 7.2 ps (assuming hyperbolic secant pulse shape) as shown in Fig. 4 (b). It should be noted that the pulse shortening is due to a dispersion compensation effect by the micro-ring resonator de-interleaver.

### 3. Experimental setup of a coherent homodyne receiver system for the CPD and MCCD

In order to demonstrate the CPD as well as the MCCD, a Mach-Zehnder interferometric homodyne detection system was built as shown in Fig. 5. In this experiment, the previous hybridly MSL was simultaneously used as a data transmitter as well as a local oscillator (LO) satisfying the required synchronization condition. For the practical SPE-OCDMA systems using synchronized MSLs, it should be noted that two separate, individual MSLs can be used where one MSL is frequency and phase-locked to the other by injection locking [5].

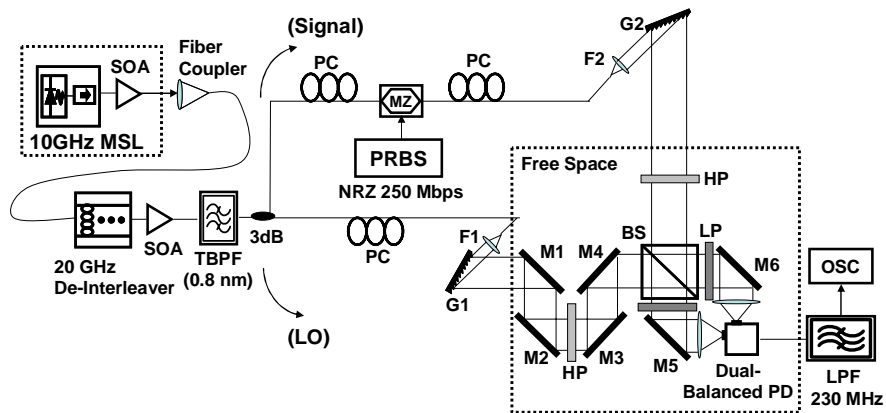


Fig. 5. Schematic of experimental setup for CPD and MCCD (TBPF: tunable bandpass filter, PC: polarization controller, F1 and F2: fiber to free space launcher, M1~M6: mirror, HP: half wave plate, LP: linear polarizer, LPF: electrical lowpass filter, OSC: oscilloscope)

After the 20 GHz de-interleaver, the filtered frequency channels of the laser output were divided into two arms of the Mach-Zehnder interferometric homodyne detection system. The signal beam imposed with NRZ modulated  $2^{10}-1$  long 250 Mb/s PRBS data is recombined with the LO beam through a free space beam splitter (BS). Subsequently, the combined beam goes to the differential balanced detection setup based on a free space dual-balanced receiver with an electrical bandwidth of 800 MHz. The diameter of the photodetectors in the balanced receiver is 0.1 mm. The saturation power of the photodetectors is 1 mW. Finally, data signals were recovered by using an electrical lowpass filter (LPF) with a bandwidth of 230 MHz in order to select only the baseband signal. It should be noted that a differential balanced detection provides suppression of the relative intensity noise (RIN) of optical sources, as well as a 3-dB sensitivity improvement as compared with direct detection.

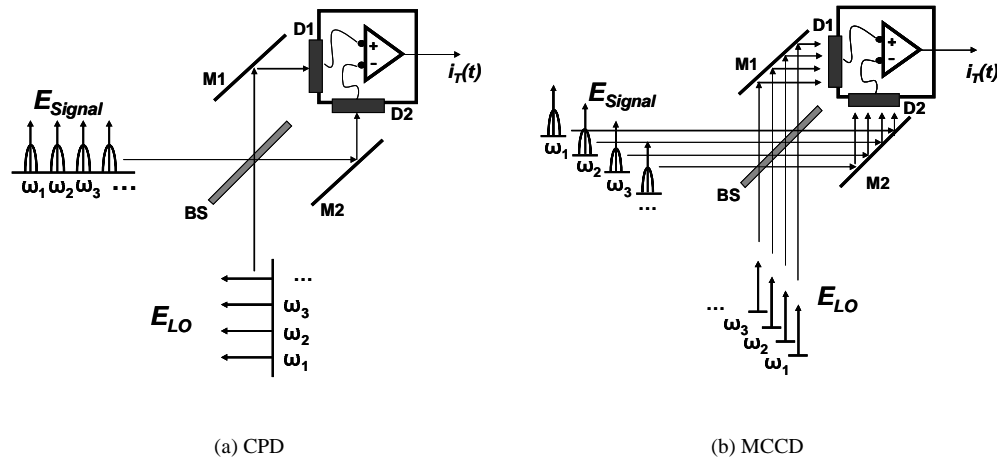


Fig. 6. Schematic of homodyne process in the CPD and the MCCD (BS: beam splitter, M1 and M2: mirror, D1 and D2: photodetector).

Figure 6 shows the schematic of the homodyne detection processes in CPD and MCCD. For the CPD experiment, the gratings (G1 and G2) in the setup were initially set up for the 0th order configuration so that the signal pulses of the entire data channels can be homodyned with the synchronized LO pulses at a single spot on the photodetector area. A free-space movable delay stage (M2 and M3) was used to control the temporal overlapping of the signal pulses with the LO pulses for the CPD experiment. On the other hand, by rotating the gratings for the 1st order configuration, MCCD was performed. In the MCCD, spatially-resolved each of the signal channels and the LO channels are individually homodyned at distinctively separate spots on the photodetector area, in the manner of channel-to-channel spatial overlap, as shown in Fig. 6(b). Each beam diameter was  $\sim 4 \mu\text{m}$ , and spatial channel separation was  $\sim 10 \mu\text{m}$ . Likewise, for MCCD each of the path lengths from the two gratings to the beam splitter (BS) was matched in order to maximize individual spatial overlapping of signal channels and LO probes at the photodetectors in the balanced receiver. As in any coherent detection process, control of the relative phase difference between the signal beam and the LO beam is crucial to realize an idealized coherent homodyne detection scheme in both CPD and MCCD.

#### 4. Comparison of the experimental results of the CPD and MCCD.

By increasing the LO power, the SNR was measured in both CPD and MCCD configurations with respect to a fixed signal power of -21.8 dBm. Figure 7 shows the SNR measurement and the corresponding eye diagrams of the CPD and MCCD. As shown in Fig. 7(b), the eye

diagram of direct detection (DD) is composed of multiple superimposed traces of the signal beam measured by blocking the LO beam after the fiber-to-free space launcher and one of the windows of the balanced receiver. The directly detected SNR was measured to be 2.6. In comparison with the direct detection, a noticeable SNR improvement was observed in both CPD and MCCD, as shown in Fig. 7(a). In MCCD, by mixing an LO power of  $\sim -10.2$  dBm with the original signal, an SNR of 9.9 was obtained from the coherently received data signals, whereas, in the CPD an LO power of more than  $\sim -6.8$  dBm was required to obtain an SNR of 9.8 from the coherently received data signals. In our experiment, the approximately 2~3 dB improvement in sensitivity obtained in MCCD compared with CPD is mainly because MCCD has an advantage in a path-length error over CPD, i.e., more stringent path-length matching in

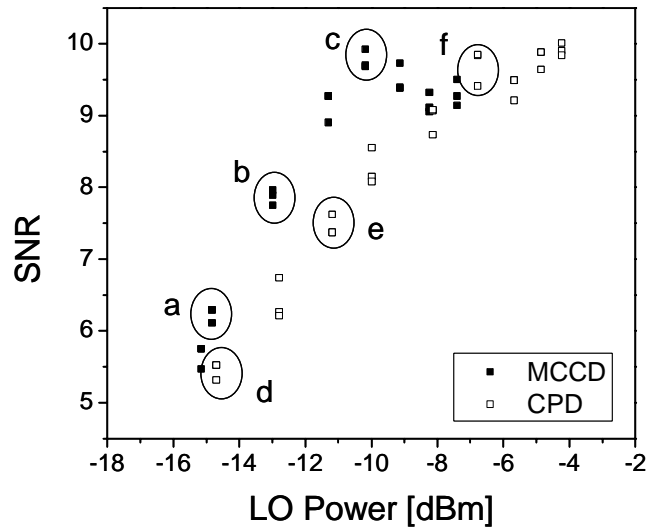


Fig. 7. (a). SNR measurement (solid symbol: MCCD, open symbol: CPD).

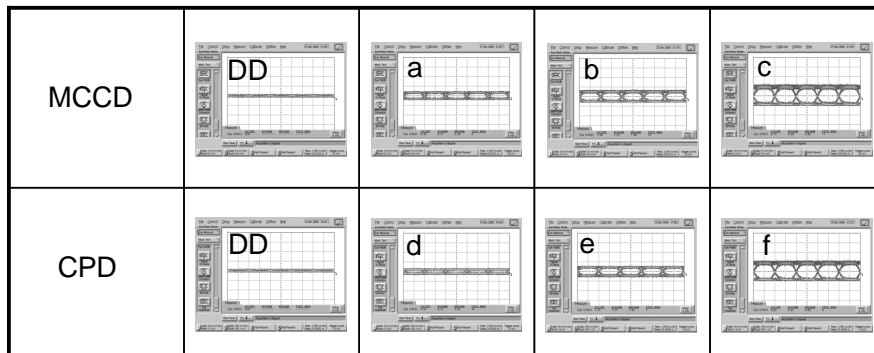


Fig. 7. (b). Eye diagrams (Scale: 10 mV/Div.)

Fig. 7. SNR measurements and the corresponding eye diagrams of CPD and MCCD

the interferometer is required for CPD. For example, a pulse duration of 7 ps can tolerate only a small path-length error such as 0.2 mm in order to acquire the 90 % temporal overlapping between the signal and the LO pulses. Whereas in MCCD utilizing spatially and spectrally resolved optical frequency combs, the channel-to-channel spatial overlapping is much less sensitive to the path-length error. In addition, In MCCD the effect of spatial shifts of the spectral channels due to the laser frequency drift is almost negligible within a coherence length of the laser source. It should be mentioned that from the estimated bit-error-rate (BER) values based on the measured SNR, error-free (BER less than  $10^{-9}$ ) coherent detection has been obtained with a LO power level of -13 dBm and -15 dBm in the CPD and the MCCD, respectively.

Figure 8 shows the LO power dependence of coherent gain in the CPD and MCCD. The measured baseband signal voltage output of the coherent detection ( $V_{CD}$ ) and the direct detection ( $V_{DD}$ ) can be given by,

$$\begin{aligned} V_{CD} &= 2 \cdot R \cdot R_L \cdot \sqrt{P_{sig} \cdot P_{LO}} \sin(\Delta\phi) \\ V_{DD} &= R \cdot R_L \cdot P_{sig} \end{aligned} \quad (1)$$

where,  $R$  is the detector responsivity,  $R_L$  is the load resistance,  $P_{sig}$  is the optical power of the signal,  $P_{LO}$  is the optical power of the LO, and  $\Delta\phi$  is the phase difference between the signal and the LO. The coherent gain can be defined as the eye opening ratio between coherent detection and direct detection, and is given by

$$G_C \equiv \frac{V_{CD}}{V_{DD}} \quad (2)$$

With a fixed signal power, the coherent gain in both CPD and MCCD has the same, square-root dependence on LO power.

$$G_C \propto \sqrt{P_{LO}} \quad (3)$$

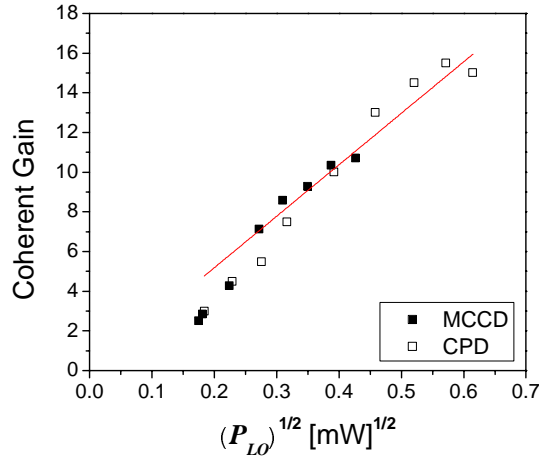


Fig. 8. Coherent gain versus LO power measurement

Our experimental results of CPD and MCCD agree well with the square-root LO power dependence of the coherent gain. A high coherent gain of over 10 dB, as well as, an SNR



improvement of over 5 dB compared with direct detection were obtained in both CPD and MCCD.

## **5. Conclusion**

In this paper, we experimentally demonstrated the performance of coherent pulse detection (CPD) and multi-channel coherent detection (MCCD) based on a single dual-balanced homodyne receiver compared with direct detection. In both detection schemes, a high coherent gain of over 10 dB, as well as an SNR improvement of over 5 dB compared with direct detection, was obtained. Our experimental results have confirmed that the coherent detection processes in CPD and MCCD are nearly the same based on a square-root LO power dependence. Nevertheless, the MCCD scheme has shown an advantage in a path-length error over the CPD scheme, revealing 2~3 dB improvement in sensitivities. Both CPD and MCCD techniques can be used for practical coherent receivers in SPE-OCDMA systems using synchronized optical frequency combs of mode-locked lasers. Consequently, the experimental results indicated that the MCCD and CPD configurations based on a single balanced receiver can both provide high (>10dB) coherent gain. Further, the MCCD receiver offers 2~3dB of SNR improvement relative to CPD at the cost of a more complex receiver configuration. Simulations suggest both approaches have the potential of strong multi-user interference rejection enabling the accommodation of a multiple users in an SPE-OCDMA system for future secure coherent communication applications.

## **Acknowledgment**

This work was supported in part by the DARPA MTO OCDMA program under contract # MDA972-03-C-0078. Any opinions, findings and conclusions or recommendations expressed in this material are those of the author(s) and do not necessarily reflect the views of DARPA.